Wind-Tunnel Results of the B-52B with the X-43A Stack

Mark C. Davis[*] and Alexander G. Sim[*]
NASA Dryden Flight Research Center, Edwards, California 93523
Matthew Rhode[†]
NASA Langley Research Center, Hampton, Virginia 23681
and
Kevin D. Johnson Sr.[‡]
Analytical Services & Materials Inc., NASA Dryden Flight Research Center,
Edwards, California 93523

A low-speed wind-tunnel test was performed with a 3%-scale model of a booster rocket mated to an X-43A research vehicle, a combination referred to as the Hyper-X launch vehicle. The test was conducted both in freestream air and in the presence of a partial model of the B-52B airplane. The objectives of the test were to obtain force and moment data to generate structural loads affecting the pylon of the B-52B airplane and to determine the aerodynamic influence of the B-52B on the Hyper-X launch vehicle for evaluating launch separation characteristics. The wind-tunnel test was conducted at a low-speed wind tunnel in Hampton, Virginia. All moments and forces reported are based either on the aerodynamic influence of the B-52B airplane or are for the Hyper-X launch vehicle in freestream air. Overall, the test showed that the B-52B airplane imparts a strong downwash onto the Hyper-X launch vehicle, reducing the net lift of the Hyper-X launch vehicle. Pitching and rolling moments are also imparted onto the booster and are a strong function of the launch-drop angle of attack.

Nomenclature

A = angle of attack polar
C_A = axial-force coefficient
C_D = drag coefficient
C_L = lift coefficient
C_l = rolling-moment coefficient
C_m = pitching-moment coefficient
C_N = normal-force coefficient
C_n = yawing-moment coefficient
C_Y = side-force coefficient
d_a = aileron position, $d_{e,r} - d_{e,l}$, deg
d_e = elevon position, $(d_{e,r} + d_{e,l})/2$, deg
$d_{e,l}$ = left elevon fin position, deg
$d_{e,r}$ = right elevon fin position, deg
d_r = rudder fin position, deg
P = proximity coefficient
R = repeat
α = angle of attack, deg
β = angle of sideslip, deg
Δ = incremental

Introduction

THREE X-43A hypersonic research vehicles (RVs) were constructed for the purpose of conducting scramjet engine research. An alternate name for the X-43A vehicle was the Hyper-X. Each vehicle was designed for one flight, and each was mounted on the front of a Pegasus® (Orbital Sciences Corporation) rocket booster in a configuration called the Hyper-X launch vehicle (HXLV). When the HXLV, the Hyper-X research vehicle (HXRV), and the adapter are combined together, the vehicle is then known as the X-43 stack. The X-43 stack was carried to the launch point by a modified B-52B airplane. Figure 1 shows the B-52B airplane carrying the HXLV stack. The captive carry of the X-43A was very similar to that of the X-15 rocket airplane (North American Aviation), which is detailed in [1].

The flight test was performed in four phases. The first phase was the captive-carry phase, during which the B-52B airplane carried the X-43A stack to the launch point. The second phase was the drop-and-boost portion of the flight, during which the Pegasus booster rocket was dropped from the B-52B airplane and boosted the HXLV to the proper flight conditions. During the third phase, the boost was completed and the HXRV separated from the booster. The fourth and final phase, from the end of the separation through the test of the engine, ended when the HXRV splashed down into the ocean. This report focuses on the captive carry and initial launch separation of the HXLV from under the right wing of the B-52B airplane. Additional X-43A project information is detailed in [2].

The three large tail surfaces, or fins, on the HXLV were used as primary control effectors. For a nominal flight, 20 deg was the maximum fin deflection. The fins were powered by thermal batteries that had a life expectancy of approximately 10 min. Approximately 2 min before launch from the B-52B airplane traveling at a Mach of 0.8, the batteries were powered up and the fin locking pins were retracted. A small-amplitude oscillation maneuver was then performed to ensure the proper operation of the fin system. Provided that all critical systems on both the booster rocket and the X-43A RV were operating properly, the HXLV would be launched. If a problem with any critical system was detected, the launch would be aborted; as part of the abort process, the fin pins would be reinserted and the B-52B airplane would return to base at a reduced speed of Mach 0.4 with the HXLV. Reinserting the fin pins before battery exhaustion was an important element of this process, because in subsonic conditions the fins were statically unstable and would be driven aerodynamically to their 51-deg mechanical stop. This would result in an off-nominal condition (nominal condition would be with the fins set at 0 deg and would result in minimal loads being imparted into the B-52B pylon) and would only occur when there was no longer power to control the fins and resist the aerodynamic forces. Although

*Aerospace Engineer, Research Engineering, P.O. Box 273, Mail Stop 2228. Senior Member AIAA.
†Aerospace Engineer, Research Engineering. Senior Member AIAA.
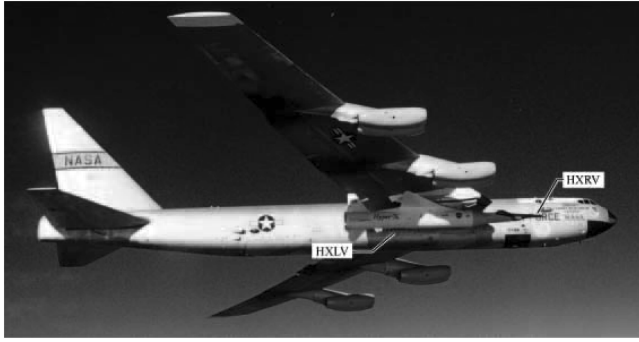‡Aerospace Engineer, P.O. Box 273, Mail Stop 2228. Senior Member AIAA.

Fig. 1 B-52B airplane carrying the Hyper-X launch vehicle stack.

Fig. 2 The 3%-scale Hyper-X launch vehicle stack model in the ViGYAN 3 by 4 ft low-speed wind tunnel.

the inability to reinsert the pins would only occur after multiple failures, the resulting structural loads into the B-52B airplane pylon were of concern.

The aerodynamics of the HXLV with full control surface deflections while in the influence of the B-52B airplane were not well understood and it was not practical to even conservatively try to calculate the aerodynamic loads. These concerns precipitated the desire to conduct a wind-tunnel test to gather aerodynamic data of the HXLV in the proximity to the B-52B airplane. A transonic test including the fabrication of a partial B-52B airplane model would have been cost-prohibitive, and there was the possibility of tunnel blockage problems rendering the results inconclusive. Also, because the return flight would be in the low-subsonic-speed range, a subsonic test was felt would be sufficient. Therefore, using an existing 3%-scale HXLV model and fabricating a partial B-52B airplane model from plastic, tests were conducted in a low-speed wind tunnel in which blockage was less of a problem and the tests were accomplished relatively quickly. The resulting aerodynamic data would not be at the same conditions as those obtained from a transonic test, but were considered conservative in the sense that the aerodynamic influences measured from a low-speed test were judged to be slightly greater than would be obtained from a test at transonic speeds.

The primary objective for the wind-tunnel test was to obtain a set of aerodynamic coefficients that could be used to calculate the structural pylon loads that results from a worst-case set of HXLV fin deflections. Thus, it was decided to conduct much of the wind-tunnel test with combinations of fin settings so that the coefficients could be directly applied to model the structural loads of the B-52B airplane pylon with the HXLV attached. As secondary objectives, force balance data were obtained with the HXLV in the wind tunnel without the B-52B airplane model (in freestream flow) to be used as a check case against other HXLV wind-tunnel tests. The freestream data were used to show the increments associated with the HXLV being in the presence of the B-52B airplane. These increments were later used to derive a simplistic model for launch separation.

Wind-Tunnel Facility Description

The ViGYAN Low-Speed Wind Tunnel is an open-circuit facility with a rectangular open-jet test section that is 3-ft tall and 4-ft wide in cross section and 5-ft long. The tunnel is powered by a variable-pitch multiblade fan located at the downstream exit. Ambient air is drawn into the inlet and through a series of antiturbulence screens and honeycombs before discharging into the test chamber. The tunnel can provide a freestream velocity up to 180 ft/s, corresponding to a Mach number of 0.16, a dynamic pressure of 38.5 psf, and a unit Reynolds number of 1.145×10^6 per foot on a standard day. The model support system allows the model attitude to be varied from -10 to $+90$ deg in pitch and -20 to $+20$ deg in yaw. Reference provides more details of the ViGYAN tunnel capabilities.

Model Description

The models used in the experiment were an existing 3%-scale HXLV model (Fig. 2) and a partial model of the B52-B airplane that was built specifically for this test. The HXLV model was originally built for the Hyper-X program by the addition of a X-43A RV and
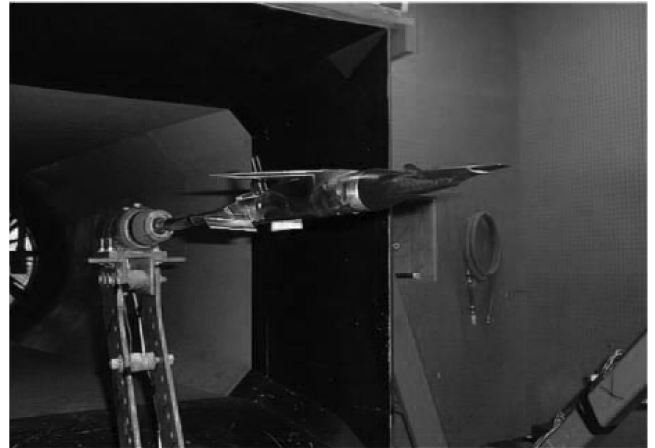

Fig. 3 Modified tailcan of the 3%-scale Hyper-X launch vehicle stack model with fin settings of 51 deg.

adapter to an existing Pegasus first stage. The model was machined from stainless steel and represents the outer mold line (OML) of the HXLV configuration, with no representation of the thermal protection system (TPS) on the wing or tail surfaces. The added X-43A RV and adapter were cast from stainless steel as one part. As originally built, the three tail surfaces on the model could deflect through a range of -20 to $+20$ deg, in 5-deg increments. Each fin had the ability to be set independently of each other. For this test, the aft fuselage was modified to allow additional deflections of ±30, ±40, and ±51 deg. Figure 3 shows the full surface deflection for the fins on the modified fuselage. Table 1 shows the control combination used in the wind-tunnel test. Surface deflections are defined as the following: d_a is aileron deflection and is equal to right elevon deflection subtracted from the left elevon deflection, d_e is elevon deflection and is equal to the left elevon added to the right elevon deflection divided by two, and d_r is the rudder deflection. The full-scale reference values are in Table 2.

Table 1 Configuration control combinations

Configuration	d_e	d_r	d_a	Definition
0	0	0	0	Zero controls
ND-NL	51	51	0	Nose down, nose left
ND-NR	51	-51	0	Nose down, nose right
NU-NL	-51	51	0	Nose up, nose left
NU-NR	-51	-51	0	Nose up, nose right
RWD-NL	0	51	-102	Right wing down, nose left
RWU-NR	0	-51	102	Right wing up, nose right

Table 2 HXLV full-scale dimensions

| Moment location	262 in.
Wing span	22.0 ft
Wing chord	8.14 ft
Wing area	145.4 ft^2

Figures 4 and 5 show the front and side views of the model in the wind-tunnel test section. As seen in Figs. 4 and 5, the B-52B airplane model was a partial representation of the B-52B carrier airplane, consisting of approximately one-half of the fuselage length and one-third of the starboard wing. The model included the pylon in the starboard wing root, along with the cutout in the wing flap for the HXLV vertical tail. The B-52B airplane model was fabricated in sections from a resinous plastic using a stereo-lithography technique. Two carbon-fiber rods were added to the wing for stiffness and the partial wing section was bonded into the fuselage. A thin fiberglass skin was added to the outer surface for a smoother surface and to add

strength to the model. An aluminum pipe was bonded into the model through the base and served as a sting support. Figures 4 and 5 show the finished product installed in the test section of the ViGYAN low-speed wind tunnel.

The 3%-scale HXLV model was mounted on a six-component strain-gage balance and attached to the model support system by way of a sting through the base of the model. The balance used for the test was the UT-56 balance. The load ranges of the balance are as follows: normal force is 50 lbf, axial force is 5 lbf, pitching moment is 50 in.-lbf, rolling moment is 8 in.-lbf, and side force is 10 lbf. The uncertainty of the balance was 0.5% full scale. The B-52B airplane model was also mounted to the model support system such that the two models moved in unison through the angle-of-attack range. For the test, the models used the coordinate system shown in Fig. 6.

The HXLV was positioned approximately 3/8 in. below the pylon to prevent contact (and damaging the balance) during the wind-tunnel tests (10-ft full scale). The lower vehicle positioning meant approximately 15% less downwash effect from the wing of the B-
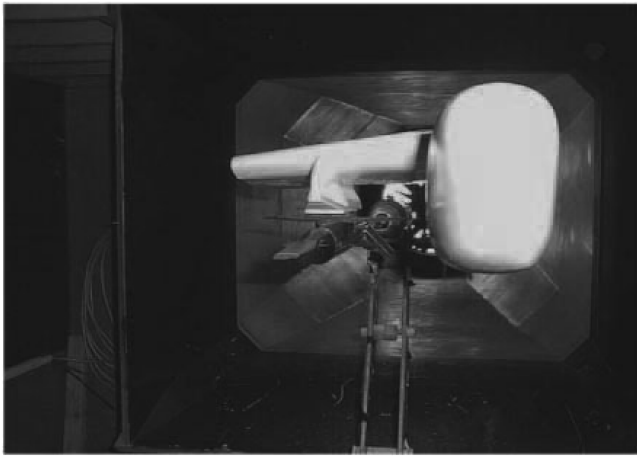
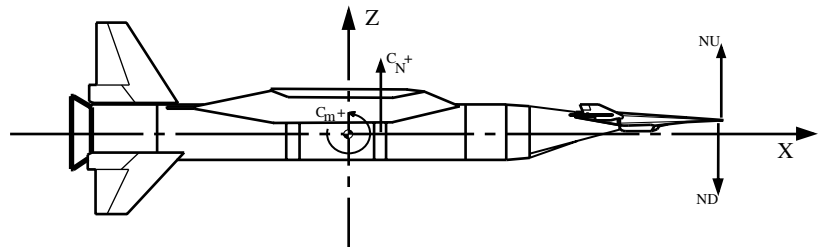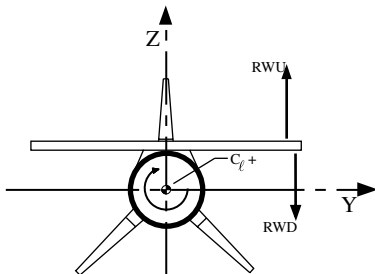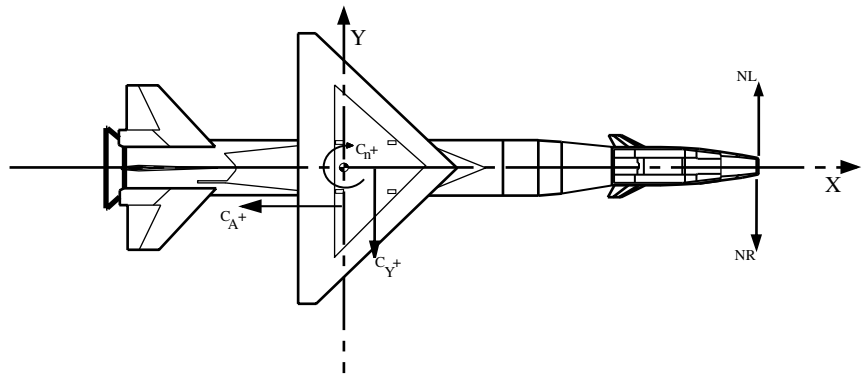**Fig. 4 Front view of the partial B-52B airplane model with the 3%-scale Hyper-X launch vehicle stack model.**

Fig. 5 Side view of the partial B-52B airplane model with the 3%-scale Hyper-X launch vehicle stack model.

HXLV surface position	
Fins	trailing edge down +
Rudder	trailing edge left +

Fig. 6 Coordinate system of the 3%-scale Hyper-X launch vehicle stack model.

Table 3 Angle-of-attack polars

Angle-of-attack polar	Break points
A1	−10, −8, −6, −4, −2, 0, 2, 4, 6, 8, 10, 12, 14, 16 deg
A2	−10, −5, 0, 5, 10 deg
A3	−2, −1, 0, 1, 2 deg

52B airplane. Additionally, this positioning allowed the center portion of the HXLV's wing to be exposed to the airflow. Both of these effects decreased the influence of the B-52B airplane onto the HXLV. In essence, the HXLV was able to produce greater lift (along with other forces and moments) in the lower position than it could attached to the pylon. Thus, the resulting aerodynamic coefficients were slightly greater in magnitude compared with pre-wind-tunnel vortex-lattice calculations. Resulting loads from these coefficients yielded a conservative structural safety analysis.

Test Description

The entire one-week test included model setup, calibration, and testing. During the wind-tunnel freestream runs, data were obtained over a limited angle-of-attack range of either ±10 or ±2 deg. Except for a couple of the initial freestream runs, the angle of sideslip was set to 0 deg.

The data runs performed used angle-of-attack polar breakpoints are found in Table 3. The test matrix, Table 4, details the 98 runs that were obtained. The data runs obtained were freestream data sets, data sets using control configurations found in Table 1, repeat data points, or were modern design of experiments (MDOE) data sets. The initial 14 runs (not shown) were setup and calibration runs conducted primarily with the air off. The scope of the test only allowed for relatively coarse breakpoints. The tests were conducted at a speed of 170 to 175 ft/s.

The primary objective for the wind-tunnel test was to obtain aerodynamic data that could be used to calculate the structural pylon loads that result from a worst-case set of HXLV fin deflections. The control surface combinations required for structural analysis are shown in Table 4. The wind-tunnel data were obtained using these specific combinations, to include any influences resulting from the combined controls. A more traditional process to obtain the data would have been to deflect each control individually and use superposition to sum the effects. However, superposition assumes the aerodynamics are independent of each other: an assumption that was avoided in this test due to the unknown influence of the B-52B airplane on the HXLV. The structural analysis was conducted for numerous flight conditions, combinations of inertial loading (maneuvering), and with the addition of gust loads. Thus, data over a large angle-of-attack range were obtained and used for the structures analysis.

Test Results

Plots of the aerodynamic coefficients, seen in Figs. 7–14, show the HXLV baseline configuration data with the controls at zero for both the vehicle in proximity to the B-52B airplane and in freestream air. The effect of the presence of the B-52B airplane is directly apparent by the increment between the two sets of data. First, the change in slope of the normal-force coefficient (Fig. 7) with angle of attack shows a 46% reduction in normal force for the vehicle while under the wing of the B-52B airplane. In effect, this means that the vehicle is not able to generate much normal force at launch until it is free from the proximity of the downwash field of the B-52B airplane. This point is further illustrated in the lift curve shown in Fig. 8. Additional calculations showed that the vehicle does not have sufficient lift at launch to climb. This is a desired effect, due to limited time, resources, and personnel, making the launch separation analysis easier. The analysis also showed a reduced possibility of recontact.

The pitching-moment coefficient (Fig. 9) shows two interesting effects. First, the angle of attack of 0 deg for pitching moment

indicates that the vehicle will tend to pitch down upon launch separation, which is a good trend for no recontact. Second, the difference in the pitching moment compared with the angle-of-attack slope is a measure of the basic longitudinal static stability. This slope difference represents approximately 20% less static margin (less longitudinal stability) when in the presence of the B-52B airplane. So as the HXLV falls away from the B-52B airplane, the static margin becomes more positive as the distance increases, until the static margin of a lone HXLV is obtained. For vehicle 2, this static margin was not a large issue because the static margin was still positive. The center of gravity for HXLV vehicle 3 was 20 in. further aft than on vehicle 2. On flight 3, the combined effects of an aft center of gravity and the proximity to the B-52B airplane yielded a vehicle slightly longitudinally unstable at launch and dictated additional separation analysis to verify if the static margin would still allow no recontact. Because of the reduced static stability for vehicle 3, the control system and control surface input was required sooner to alleviate the potential problem.

Another parameter of interest was the rolling-moment coefficient (Fig. 10) caused by the low roll inertia of the HXLV and the rolloff at launch for previous Pegasus rockets dropped from the B-52B. The data show that the vehicle will be induced to roll positive (clockwise direction) at launch angles of attack below approximately 2 deg. Because of longitudinal stability discussed in the previous paragraph and an induced roll at launch, the timing to activate the HXLV control system was changed from approximately 0.5 s after launch to approximately 0.2 s for vehicle 3. The vehicle would drop approximately 5 ft before control activation on flight 2, and 2 ft for flight 3.

The yawing-moment coefficient (Fig. 11) is normally near zero unless the fin is deflected, because of the HXLV vertical tail (fin) being located behind the pylon strut. The side-force coefficient (Fig. 12) generated shows that there is a significant influence in the presence of the B-52B airplane. Even so, an analysis of drag (Fig. 13) shows that angles of attack other than near zero show less overall drag. Also, axial force (Fig. 14) follows the same trend as drag, with a decrease in overall axial force with angles of attack other than zero.

A limited evaluation of large control deflections within proximity to the B-52B airplane was also conducted. Data were obtained for HXLV fin deflections of 0, 20, 30, 40, and 51 deg. All data were obtained near zero angle of attack and were for nose-up elevon deflection, nose-left rudder, or right-wing-down aileron. The results showed that the individual fins produced their maximum effectiveness around 30-deg deflection and were effectively stalled by the time the 51-deg mechanical stop was reached. The elevon maximum pitching moment occurred at the 30-deg deflection and was at 65% of maximum for 51 deg of elevon deflection. The rudder maximum yawing-moment increment occurred at the 30-deg deflection and was 76% of maximum at 51 deg of rudder deflection. The aileron incremental rolling-moment maximum occurred at 60-deg deflection (total differential elevon angle definition) and was reduced to 84% of the maximum value at 102 deg or 51-deg individual deflection of the left and right fin. Although the primary control effectiveness decreased beyond 30 deg of fin movement, as expected, the drag continued to increase until at 51 deg it was approximately twice the drag at 30 deg.

Separation Model

Before flight 3, the wind-tunnel data had only been used for structural analysis studies. The concern of launching flight 3 in a slightly longitudinally statically unstable condition was that the vehicle might be able to pitch and roll enough to strike the vertical tail on the pylon. Thus, a simple launch separation model was developed. The primary data used were the same as presented in Figs. 7–14. The increments in the aerodynamic coefficients between the HXLV in freestream and in the presence of the B-52B airplane were used to define a set of incremental coefficients that were added to the corresponding total coefficients in a batch simulation. However, these incremental coefficients only define one location 10 in. (0.833 ft) below the pylon. For the simulation, it was necessary to compute a proximity coefficient to model how the influence of the B-

Table 4   Test matrix: X-43A/B-52 hardover fins aerodynamics in the ViGYAN 3 by 4 ft low-speed wind tunnel

Sequence	Run	Configuration	α	β	$d_{e,l}$, deg	$d_{e,r}$, deg	d_r, deg	d_e, deg	d_a, deg	Comments
1	16	HXLV freestream A1	0	0	0	0	0	0	0	Database comparison check, R
2	15		4	0	0	0	0	0	0	
3	17		−4	0	0	0	0	0	0	
4	18		0	0	10	10	0	0	0	
5	19		0	0	−10	10	0	0	20	
6	20		0	0	0	0	10	0	0	
7	33, 40, (73)	HXLV and B-52 A2	0	0	0	0	0	0	0	HXLV and B-52, zero controls
8	34, 41, 46, (76)		0	0	0	0	51	0	0	NL
9	35, (74)		0	0	0	0	−51	0	0	NR
10	36, 39, (50, 71)		0	0	−51	−51	0	−51	0	NU
11	32, (55, 72)		0	0	51	51	0	51	0	ND
12	37, (59)		0	0	51	−51	0	0	−102	RWD
13	38, 62, 68		0	0	−51	−51	51	−51	0	NL, NU
69	80		0	0	−51	51	0	0	102	LWD
14	21, 22, 23, 96, 97, 98	HXLV freestream A1	0	0	0	0	0	0	0	HXLV in freestream flow, R(6)
15	24, 30		0	0	0	0	51	0	0	R
16	25		0	0	0	0	−51	0	0	
17	26		0	0	−51	−51	0	−51	0	
18	27, 31		0	0	51	51	0	51	0	R
19	28		0	0	51	−51	0	0	−102	
20	29		0	0	−51	−51	51	−51	0	
65	95		0	0	−51	51	0	0	102	
21	42	HXLV and B-52 A3	0	0	0	0	20	0	0	Aerodynamic trends, rudder
22	43, 60		0	0	0	0	30	0	0	R
23	44, 45		0	0	0	0	40	0	0	
24	46		0	0	0	0	51	0	0	
25	47		0	0	−20	−20	0	−20	0	Aerodynamic trends, positive elevon
26	48		0	0	−30	−30	0	−30	0	
27	49		0	0	−40	−40	0	−40	0	
28	50		0	0	−51	−51	0	−51	0	
29	52		0	0	20	20	0	20	0	Aerodynamic trends, negative elevon
30	53, 61		0	0	30	30	0	30	0	R
31	54		0	0	40	40	0	40	0	
32	55		0	0	51	51	0	51	0	
33	56		0	0	20	−20	0	0	−40	Aerodynamic trends, aileron
34	57		0	0	30	−30	0	0	−60	
35	58		0	0	40	−40	0	0	−80	
36	59		0	0	51	−51	0	0	−102	
38	63	HXLV and B-52 A2	0	0	−51	−51	−51	−51	0	NR, NU
37	38, 62, 68		0	0	−51	−51	51	−51	0	NL, NU (repeat sequence 13)
40	64, 69		0	0	51	51	−51	51	0	NR, ND
39	65		0	0	51	51	51	51	0	NL, ND
41	78		0	0	−51	51	−51	0	102	NR, LWD
42	79		0	0	51	−51	51	0	−102	NL, RWD
51	66		0	0	−51	51	51	0	102	NL, LWD
52	67		0	0	51	−51	−51	0	−102	NR, RWD
43	70	HXLV and B-52	−5	0	0	0	0	0	0	MDOE, block 2
44	71		0	0	−51	−51	0	−51	0	
45	72		0	0	51	51	0	51	0	
46	73		0	0	0	0	0	0	0	
47	74		0	0	0	0	−51	0	0	
48	75		5	0	0	0	0	0	0	
49	76		0	0	0	0	51	0	0	
50	77		0	0	0	0	0	0	0	
53	83	HXLV and B-52	0	0	0	0	0	0	0	MDOE, block 1
54	84		3	0	−30	−30	−30	−30	0	
55	85		3	0	30	30	30	30	0	
56	86		0	0	0	0	0	0	0	
57	87		−3	0	−30	−30	−30	−30	0	
58	88		0	0	0	0	0	0	0	
59	89		−3	0	30	30	30	30	0	
60	90		−3	0	30	30	−30	30	0	
61	91		3	0	−30	−30	30	−30	0	
62	92		0	0	0	0	0	0	0	
63	93		−3	0	−30	−30	30	−30	0	
64	94		3	0	30	30	−30	30	0	

52B airplane varied with separation distance. This was accomplished by using a vortex-lattice program to calculate the lift slope as a function of distance by using a planar model of the HXLV under a planar model of a B-52B airplane wing (without the pylon). A factor was then derived using the inverse of the increment in the lift-curve slope normalized to unity at the 10-in. separation. A coefficient was calculated at discrete points between 0 and 5 ft below the pylon. Below 5 ft of separation distance, the factor was linearly ramped to zero by the 20-ft point. Justifications for early influence termination were that the HXLV would not hold its longitudinal position directly under the wing of the B-52B airplane (because the B-52B airplane would continue traveling forward as the HXLV would, because of
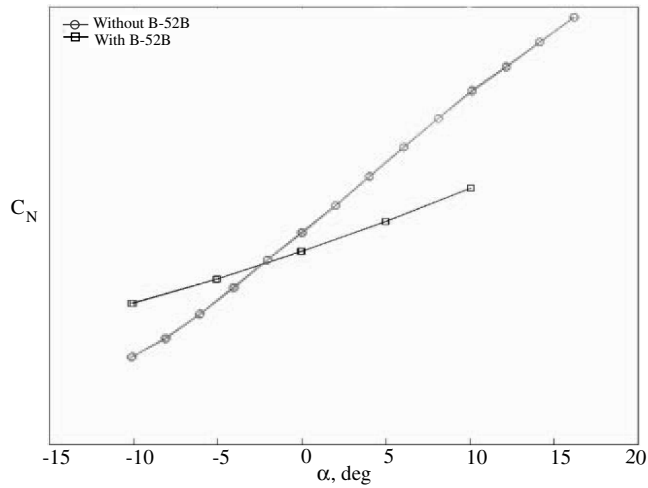
Fig. 7 Hyper-X launch vehicle normal-force coefficient with and without the influence of the partial B-52B airplane model.
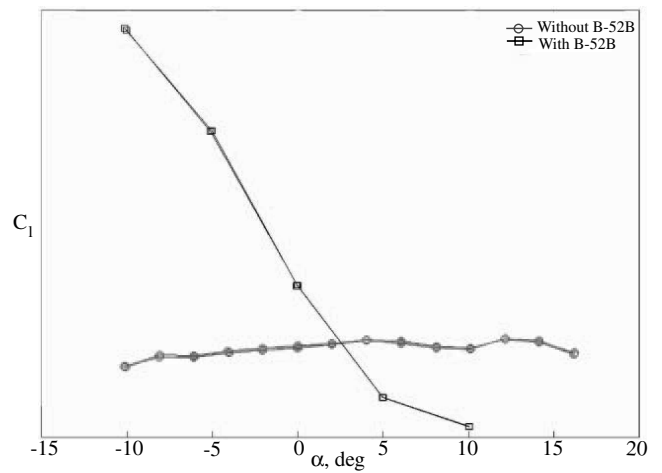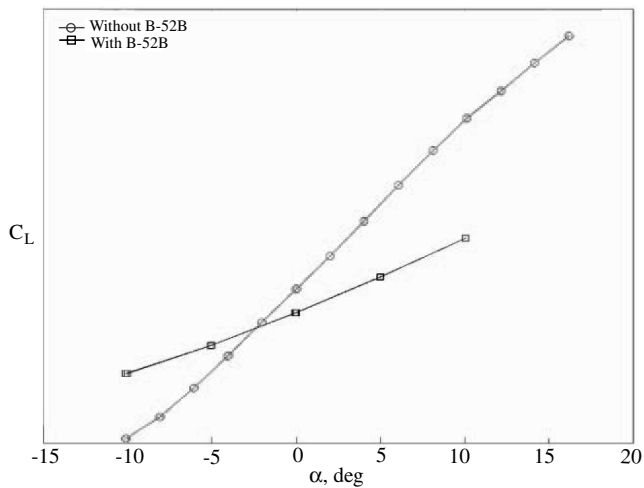

Fig. 8 Hyper-X launch vehicle lift coefficient with and without the influence of the partial B-52B airplane model.
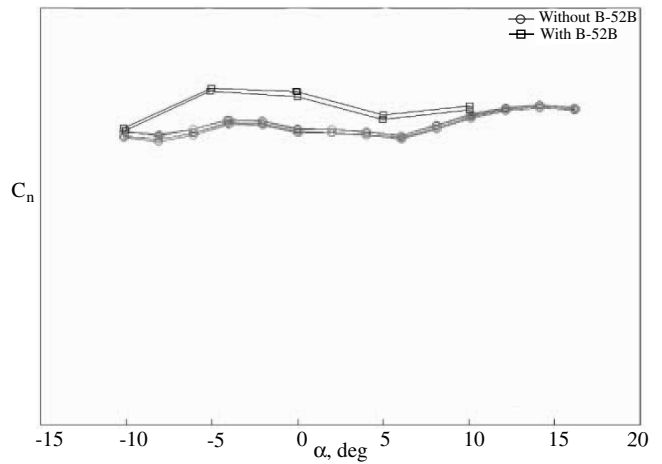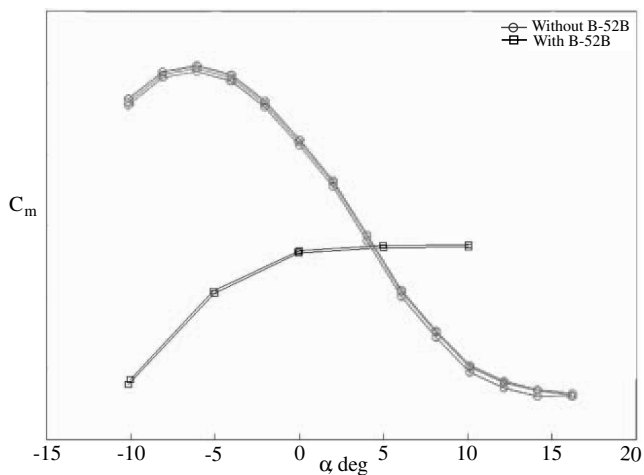

Fig. 9 Hyper-X launch vehicle pitching-moment coefficient with and without the influence of the partial B-52B airplane model.
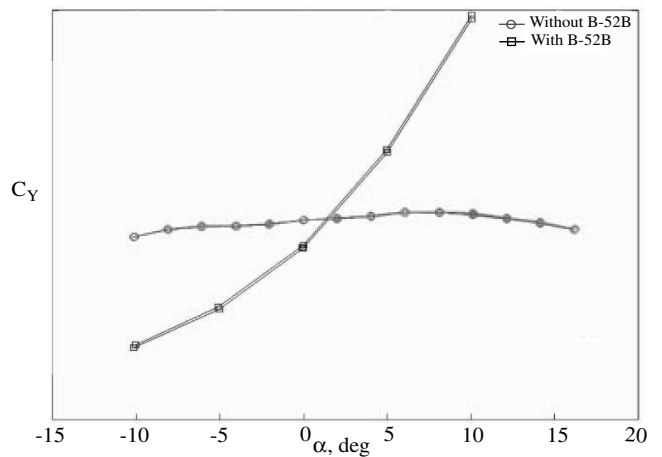

Fig. 10 Hyper-X launch vehicle rolling-moment coefficient with and without the influence of the partial B-52B airplane model.

Fig. 11 Hyper-X launch vehicle yawing-moment coefficient with and without the influence of the partial B-52 airplane model.


Fig. 12 Hyper-X launch vehicle side-force coefficient with and without the influence of the partial B-52 airplane model.

of the batch simulation showed the resulting pitch rate increasing to approximately 1 deg /s after launch. This small pitch rate was not a safety concern.

Conclusions

A test was conducted in a low-speed wind tunnel to determine the effectiveness of the Hyper-X launch vehicle fins in the proximity of
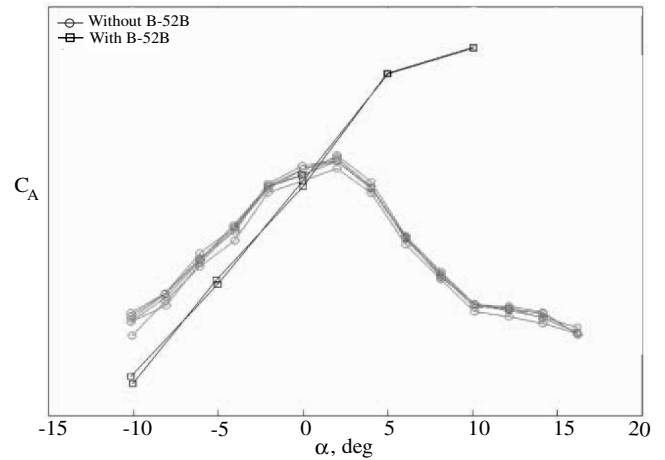
drag, rapidly translate aft) and that the first 5 ft of separation were of primary interest. The resulting proximity P factor is multiplied by each of the incremental aerodynamic coefficients. It is considered conservative because its starting value is greater than one. In reality, it is likely less than unity when in contact with the pylon. The results
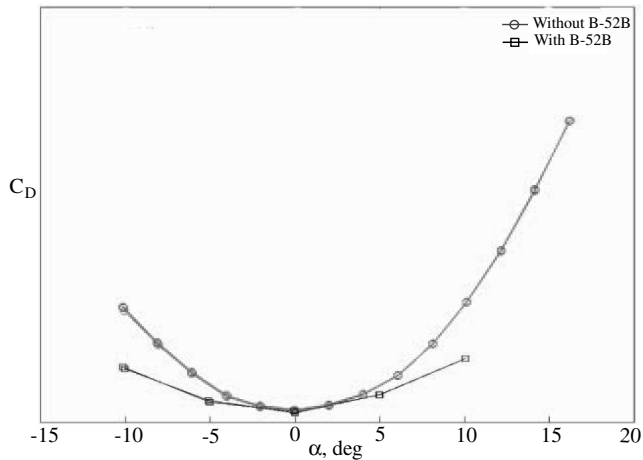
Fig. 13 Hyper-X launch vehicle drag coefficient with and without the influence of the partial B-52 airplane model.

Fig. 14 Hyper-X launch vehicle axial-force coefficient with and without the influence of the partial B-52 airplane model.

the B-52B airplane. Test parameters included worst-case scenarios of the fins going to their hardover stops of 51 deg.

The test obtained aerodynamic coefficients for use in a separation model. The data were obtained in proximity to the B-52B airplane model and then a proximity factor was developed to allow for varying separation distances and their influences to be incorporated in a simulation. The test data were used to formulate a simple launch separation model. The launch separation model was then used to examine the possibility of recontact and showed that recontact was not likely because of the decreased lift capability demonstrated while the model was in the influence of the B-52B airplane.

Testing in the low-speed wind tunnel used the configuration of an existing 3%-scale Hyper-X launch vehicle model and a plastic model of a partial B-52B airplane. These models were used to obtain the aerodynamic influence on load data into the launch pylon.

References

[1] Adolph, C. E., Allavie, J. E., and Bock, C. C., Jr., "Flight Evaluation of the B-52 Carrier Aircraft for the X-15," U.S. Air Force Flight Test Center Rept. TR-60-33, Edwards AFB, CA, Sept. 1960.

[2] Freeman, D., Reubush, D., McClinton, C., Rausch, V., and Crawford, L., "The Hyper-X Program," NASA TM-97-207243, 1997.

[3] Dominguez, K., Graham, A. B., and DeLoach, R., "Development of an MDOE Compliant Control System in the ViGYAN Low-Speed Wind Tunnel," AIAA Paper 2001-0169, 2001.

M. Miller
Associate Editor